# NOVEL MOTORS AND CONTROLLERS FOR HIGH PERFORMANCE ELECTRIC VEHICLE WITH 4 IN-WHEEL MOTORS

Masayuki Terashima*, Tadashi Ashikaga Takayuki Mizuno (Meidensha Corporation)

Kazuo Natori, Noboru Fujiwara, Masayuki Yada (Tokyo Electric Power Company)

*Product Development Laboratory, Meidensha Corporation 2-1-17 Ohsaki Shinagawa-ku Tokyo 141, Japan

*Abstract*

*We have, in accordance with new concepts, undertaken the development of a high-performance electric motor vehicle, designated as the IZA. The main performance features of the IZA are a maximum speed of 176 km/h, a range of 548 km per charge at a constant speed of 40 km/h, and acceleration from 0 to 400 m in 18 seconds. We have developed a direct driving in-wheel motor and controller in order to achieve high performance characteristics. The in-wheel motor is composed of an outer rotor with a rare earth permanent magnet (Sm-Co) and an inner stator. The motor drive controller consists of a 3-phase inverter and a microprocessor-based controller. The maximum output and maximum torque of each total drive system, including motor and inverter, are 25 kW and 42.5 kgm, respectively, and the total efficiency of the drive system is over 90% at the rated speed. The performance of the motor, controller, and drive system have been confirmed by numerous simplex and vehicle transit tests. This paper describes the design concepts, configuration, and performance of the motor, controller, and drive system developed for this high performance electric vehicle.*

## 1. Introduction

Many types of electric vehicles have been developed and practically operated. In Japan, for example, from 1971 to 1976, EVs which were epochal at that time were developed under a major EV project sponsored by the Ministry of International Trade and Industry [1]. However, previous electric motor vehicles have not been comparable with gasoline-driven vehicles as regards performance and cost, and infrastructural facilities such as battery chargers were not provided. These are the main reasons why electric vehicles never came into widespread use. Recently, the development of electric vehicles has been promoted in many projects throughout the world, largely owing to recognition of the vital importance of global environmental problems [2] [3].

In order to radically change conventional views concerning the limitations of electric vehicles, we have, in accordance with new concepts, undertaken the development of a high-performance electric motor vehicle, designated as the IZA. The basic concept of the IZA project is the realization of a high performance electric vehicle with an optimal balance of maximum speed, acceleration performance and traveling range per charge. The main performance characteristics of the IZA are a maximum speed of 176 km/h, a range of 548 km per charge for a constant speed of 40 km/h, and acceleration from 0 to 400 m in 18 seconds [4]. These performance characteristics are comparable with those of gasoline-driven vehicles. The high performance of the IZA has been made possible by a newly developed motor and controller in addition to vehicle body improvements such as reducing the body weight and air resistance as well as the use of a nickel cadmium battery. The salient characteristics of the drive system are as follows [5], [6].

(1) Four motors drive the wheels directly without mechanical gear.

(2) Motors are synchronous motors with permanent magnets and are placed inside wheels.

(3) Controlled current inverters are employed for each motor. The in-wheel motor is composed of an outer rotor with rare earth permanent magnets (Sm-Co) and an inner stator. The motor drive controller consists of a 3-phase inverter and a microprocessor-based controller. By adopting IGBT as the switching power devices, increased switching frequency and high torque control are made possible even at high motor speeds. Field weakening control was employed in this controller to increase the motor overspeed rating. The maximum output and maximum torque of each total drive system, including the motor and inverter, are 25 kW and 42.5 kgm, respectively, and the total efficiency of the drive system is over 90% at the rated speed. The performance of the motor, controller, and drive system have been confirmed by numerous simplex and vehicle transit tests.

The purpose of the present paper is to describe the design concepts, configuration, and performance of the motor, controller and drive system developed for this high performance electric vehicle.

## 2. Overview of IZA

Table 1 shows the principal specifications and main performance as confirmed by tests. In order to realize the target performance, the basic design approach was as follows.

(1) Aluminum chassis and FRP (carbon fiber reinforced plastic) body were employed to reduce the weight of the vehicle.

(2) Models with the proposed vehicle shapes were fabricated and tested in order to minimize air resistance. The value of the air resistance coefficient Cd is 0.19.

(3) NiCd batteries specially developed for use in electric vehicles were employed as the power source. The capacity of

| Body Size | | Motor and Inverter | |
|---|---|---|---|
| Length | 4.87m | Rated output(cont.) | 6.8kW |
| Width | 1.77m | Maximum output | 25kW |
| Height | 1.26m | Maximum torque | 42.5kg·m |
| Curb Weight | 1,573kg | Maximum speed | 1,540rpm |
| Passengers | 4 | Motor weight | 33kg |
| Range per charge | | Inverter weight | 22kg |
| 40km/h constant | 548km | Battery | |
| 100km/h constant | 270km | Type | NiCd |
| Maximum speed | 176km/h | Capacity | 100Ah |
| Acceleration | | source voltage | 288V |
| 0-400m | 18.05s | Number | 24 |
| 0-40km/h | 3.47s | Weight | 531kg |
| Maximum upward slope | 32% | | |

TABLE 1   Principal Specifications and Main Performance of IZA

| | Speed (km/h) | Motor Speed (rpm) | Output (kW) | Torque (kg·m) | Rated time | Kind of operation |
|---|---|---|---|---|---|---|
| A | 180 | 1,540 | 11.7 | 7.2 | 3 min | Maximum speed |
| B | 15 | 128 | 5.6 | 42.5 | 20 s | Maximum torque |
| C | 120 | 1,030 | 20.0 | 19.0 | 30 s | Passing other cars |
| D | 180 | 1,283 | 6.8 | 5.2 | cont. | Continuous rated torque |

TABLE 2   Ratings of motor

each battery is 100Ah and twenty-four batteries are installed. (4) Four driving motors are installed, one inside each of the four wheels. In-wheel motors were adopted because, firstly, transmission and differential gears are eliminated and efficiency is improved, and secondly, more batteries can be installed in the space which would otherwise be occupied by the transmission and differential gear.

(5) A miniaturized synchronous motor with an outer rotor structure was developed, and a high-performance rare-earth (SmCo) permanent magnet was employed to improve the efficiency of the motor.

(6) A newly developed inverter was used for the power source of each of the four motors. The inverter is of the sinusoidal current controlled type and is designed to control motor torque over a wide speed range and reduce the harmonic losses of the motor.

## 3. Drive motor
### 3.1 Required motor ratings and design concepts

Table 2 shows the motor ratings which were established in order to achieve the above-mentioned performance characteristics. Row A indicates the maximum speed of the IZA, row B the maximum torque required for rapid acceleration when starting, row C the torque required for passing other cars at a speed of 120 km/h, and row D the continuous rated torque at a speed of 150 km/h. These torque-speed characteristics must be realized under the condition that the motors are installed within the wheels.

Figure 1 shows a cross-sectional diagram of the in-wheel motor. This is a synchronous motor with an outer rotor structure composed of a rotor employing a high-performance rare-earth (SmCo) permanent magnet for the field (12-pole). An absolute encoder is employed in the detector which locates the positions of the magnetic poles of the rotor.

Although we fabricated and experimented with both water cooled and self-cooled types of motors, the motor finally employed in the IZA is self-cooled, and requires no special cooling apparatus.

### 3.2 Effects of magnetic saturation

In a synchronous electric motor with a field system employing a permanent magnet, the steady torque characteristics and cogging torque are also greatly influenced by the magnetic flux density distribution in the gap of the magnet. Therefore, the magnetic circuit was analyzed as follows.

In the present motor, as indicated in Table 2, a maximum torque equivalent to approximately 8 times the continuous steady torque is required, and therefore a high coercive force magnet (SmCo) with no danger of demagnetization is employed, and is supplied with a large current. Hence, the effects of local magnetic saturation due to armature reaction must be considered.

Figure 2 shows the results of magnetic field analysis by the finite element method. Figure 2(a) indicates the magnetic flux distribution due to the magnet alone (under no load), (b) the magnetic flux distribution due to the armature current alone, and (c) the resultant magnetic flux distribution (under load).

Under a load, since the armature magnetomotive force is superposed upon the principal magnetic flux due to the magnet, the magnetic flux density in each portion increases in the teeth on the right-hand side of the pole. That is, when current flows, the magnetic flux deviates toward the direction of rotation, which tends to increase the magnetic flux density in the core teeth. Therefore, in the case of the present motor, if a large current flows, then the teeth are saturated, which decreases the principal magnetic flux, thereby distorting the linearity of the torque-current relation. The torque-current characteristic is shown in Figure 3. Here, the broken line represents the linear relation in an unsaturated state, while the curve plotted with a solid line represents the torque deduced from the analytical results. Actual measured values, indicated by circles, agree well with the analytically deduced curve. This figure shows that effects of armature reaction are manifested after the torque has risen above 5 times the rated value, and the torque displays a tendency toward saturation. However, we confirmed that the motor and inverter possess sufficient margin to cope with the increase in motor current associated with saturation.
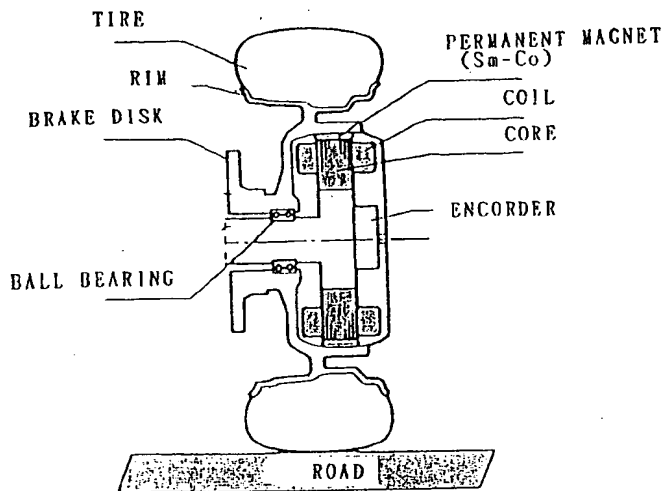
Fig.1 Cross sectional diagram of in-wheel motor



(a) Flux distribution
due to magnets alone

(b) Flux distribution
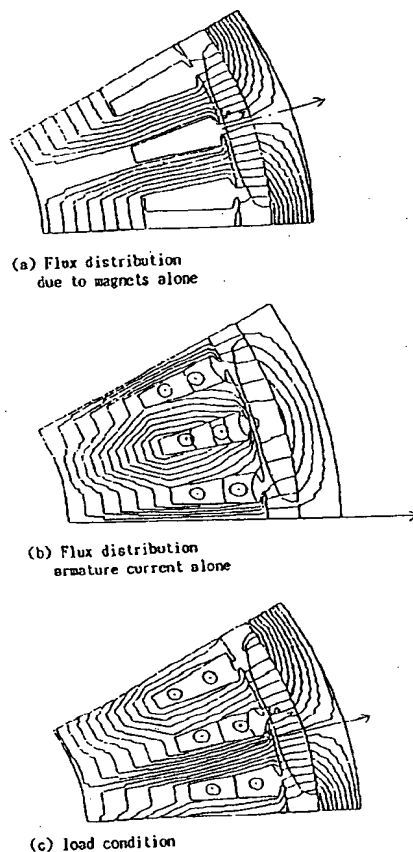armature current alone

(c) load condition
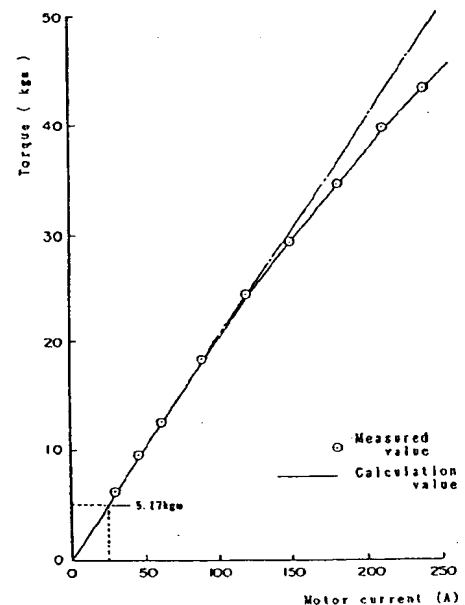
Fig.2 Result of magnetic field analysis



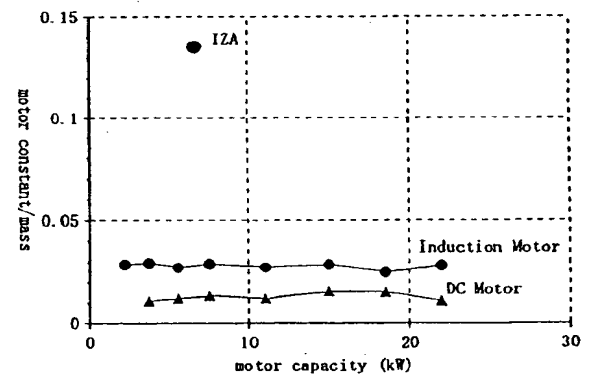Fig.3 torque vs motor current characteristics



Fig.4 Motor constant/mass of IZA compared with common motors

Excellent motor is high power small size and high efficiency.
Motor constant $K_M$ defined as following equation is mostly
used for evaluate performance of motors.

$$K_M = \tau / \sqrt{W_c}$$

where, $\tau$ : output torque, Wc: copper loss
The motor efficiency is given by following equation using

22

motor constant taking only copper loss in consideration.

$$\eta = \frac{1}{1+P/(K_M\omega)^2}$$

Figure 4 shows motor constant/weight of ordinary DC motor and induction motor, and that of IZA is plotted. The figure shows performance of IZA is excellent comparing with ordinal motors. If an induction motor of 7.5kw were used in stead of the developed motor, then, efficiency at designed point D (1283rpm, 6.8kw) would be about 6 point lower, and the weight of the motor would be about 2 times larger.

## 4. Drive Control

In the preceding Chapter, we described the motor characteristics required to satisfy the specifications of the IZA. However, these characteristics are realized not only through motor capability but also by the entire drive system, which must possess sufficient capability to supply the sinusoidal motor current. In other words, the entire drive system, including the inverter and battery, must be analyzed in addition to the motor. This chapter shows how the following problems concerning the drive system of the IZA have been dealt with.

(1) Torque-speed characteristics design, taking the motor, inverter and battery into consideration

(2) High response sinusoidal current control

(3) Attainment of a vehicle speed of 180 km/h

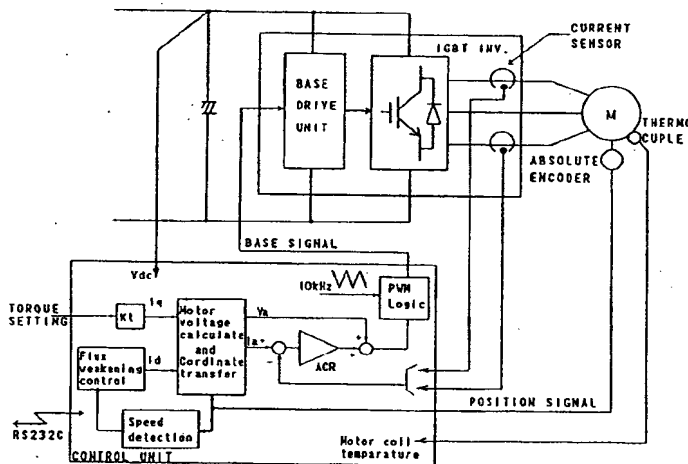(4) Design and simulation relating to traveling range per charge



Fig.5 Block diagram of the motor controller

### 4.1 Inverter and motor control

One motor controller is provided for the motor in each of the four wheels. Overall control of the vehicle is effected by the vehicle controller, which issues commands to the motor controllers.

Figure 5 shows the configuration diagram of the motor controller. The motor controller receives command values for the torque corresponding to the accelerator of the vehicle, and controls the inverter. The controller outputs state monitoring signals specifying the motor speed, the motor current, the temperature of the stator winding, and the DC voltage of the inverter. Alarm signals emitted by the motor controller are transmitted by serial communication through an RS232C interface to the vehicle controller. These control functions and the current coordinate transformations to be described below are processed by the CPU (8096).

Adoption of IGBTs as the switching power devices of the inverter permitted increased switching frequency and reduced harmonic losses in the motor. Motor currents are controlled as follows. The permeance of the driving motor is equivalent to that of a cylindrical field type motor, because the magnets are installed on the rotor surface. For this reason, the inductance of the d-axes and q-axes are equal, and the voltage and torque are given by the following equations (1) and (2), respectively, while the transformation from 3-phase to 2-phase is expressed by equation (3).

$$\begin{bmatrix} v_d \\ v_q \end{bmatrix} = \begin{bmatrix} R+Lp & -n\omega L \\ n\omega L & R+Lp \end{bmatrix} \begin{bmatrix} i_d \\ i_q \end{bmatrix} + \begin{bmatrix} 0 \\ n\omega\lambda \end{bmatrix} \quad (1)$$

$$T = k_t\lambda i_q \quad (2)$$

$$\begin{bmatrix} i_d \\ i_q \end{bmatrix} = \frac{2}{3} \begin{bmatrix} \cos\theta & \cos(\theta-2/3\pi) & \cos(\theta+2/3\pi) \\ -\sin\theta & -\sin(\theta-2/3\pi) & -\sin(\theta+2/3\pi) \end{bmatrix} \begin{bmatrix} i_a \\ i_b \\ i_c \end{bmatrix}$$

$$(3)$$

Here, the notations used are as follows.
R: resistance of winding   Ld, Lq: self-inductance of d- and q-axes   $\lambda$ : number of flux interlinkages of stator winding   n: number of pole pairs   $\omega$ : angular velocity   Kt: torque constant   p: differential operator   $\theta$ : angle between d-axis and phase a-axis

From equations (1) and (2), it is obvious that only the q-axis current determines the magnitude of the torque, which is unaffected by the d-axis current. The motor controller receives a torque command corresponding to the angle of the accelerator pedal, and creates a q-axis current command iq* which is proportional to the torque command, then, iq* is converted to motor current commands by using the inverse transformation of equation (3), where the rotor position $\theta$ is obtained from the absolute encoder. The analog current controller regulates the motor AC currents to ensure their agreement with these commands. Although phase lag is prone to occur in AC control systems, especially during high velocity operation, the AC motor current must be strictly controlled in the present system. We employed induced voltage compensation, whereby the instantaneous motor voltage is calculated using the detected rotor position and added to the output of the current controller [7].

The current vector of the motor is constantly maintained in orthogonality with the rotor flux vector by the controlled current source type sinusoidal PWM inverter as mentioned

BEST AVAILABLE COPY

above, and therefore the motor output torque is proportional to the motor current. However, the motor terminal voltage increases in proportion to the motor speed in this type of control system, therefore, the motor speed cannot increase above the rated speed determined by the inverter voltage limit. It is possible to design the system so that the motor voltage does not exceed the maximum voltage limited by the battery, but such a design would not be economical because a large motor size would be necessary. This is the problem entailed by the use of permanent magnet type motors in electric vehicles. We employed field weakening control in the present controller in order to resolve this problem.

In equation (1), $n\omega\ \lambda$ is the induced voltage, and if the linkage flux $\lambda$ is controlled by regulating the d-axis current id, then Vq can be adjusted. By making id negative, the value of Vq can be decreased and the terminal voltage $V_1$ shown in equation (4) can also be adjusted to a smaller value.

$$v_1 = \sqrt{v_d^2 + v_q^2} \qquad (4)$$

From equation (2), since the torque is not related with id, if the value of iq is held constant, then $V_1$ alone can be reduced by decreasing id, without changing the torque. In field weakening control, since the motor current is increased in accordance with the flow of the id current, the copper losses in the motor will also increase. Hence, this control is effected when the speed exceeds 1280 rpm (row D in Table 2). In practice, the motor current in the IZA does not increase unduly even under field-weakening control, and continuous drive at about 180 km/h is possible.

4.2 Overall characteristics of drive system

The maximum output torque of the driving system for each rotation speed under ordinary control conditions can be determined by the following procedure. The relation between the battery output, motor output and losses is expressed by the following equation (5).

$$E_{dc}I_{dc} - I_{dc}R_b = W_{INV} + W_{IM} + 3I_aE_0 \qquad (5)$$

The last term $3I_aE_0$ of above equation is the output of the motor, including mechanical losses, and the notations are as follows.

$W_{INV}$ : Inverter loss, $W_{IM}$ : Motor loss, $V_0$: Open circuit voltage of battery  $R_b$: Internal resistance of battery, $I_{dc}$: DC current, $E_{dc}$: DC voltage $V_a$: Output voltage of inverter, $I_a$: Motor current,  $E_0$: Induced voltage of motor, $R_m$: Resistance of motor winding

Inverter losses consist of steady-state losses and switching losses, which can be approximated as functions of the motor current Ia by the equation

$$W_{INV} = K_1I_a^2 + K_2I_a \qquad (6)$$

where $K_1$ and $K_2$ denote inverter loss coefficients.
The motor losses are expressed by the following equations, since both the primary copper loss and stray loss are proportional to $I_a^2$. Here, $R_a$ denotes the equivalent resistance of the motor, taking stray losses into consideration.

$$W_{IM} = R_aI_a^2 \qquad (7)$$

On the assumption that the power factor is one (1.0), the relation between Ia and Idc is given by the following equation (8), where $\mu$ denotes the control factor of the inverter.

$$I_{dc} = \frac{3}{2\sqrt{2}}\mu I_a \qquad (8)$$

If one sets $\mu = 1$ in the above equation, then one can determine the maximum output current for each rotational speed, as expressed by equation (9), and by subtracting the no-load loss, the maximum output torque for each rotational speed can be calculated.

$$I_a = \frac{6\sqrt{2}\,\mu V_0 - 8\,(K_2 + 3E_0)}{9\mu^2 R_b + 8\,(K_1 + R_a)} \qquad (9)$$

Here, $E_0 = K_n/K_t \cdot n$
On the other hand, the maximum possible power in the regeneration control mode is limited by the maximum battery power or the maximum inverter voltage. Denoting the maximum regenerative power of the battery by Pdc, the maximum current in the regenerative mode can also be derived, as expressed by the following equation (10).

$$I_a = \frac{(3E_0 - K_2) \pm \sqrt{(3E_0 - K_2) - 4\,(K_1 + R_a)\,P_{dc}}}{2\,(R_a + k_1)} \qquad (10)$$

Figure 6 shows the maximum torque characteristic with respect to the rotational speed of the present motor when the battery is fully charged. The maximum torque in the low-speed region during driving operation is limited by the maximum permissible current (240 A) of the inverter, and is equal to 42.5 kgm. In this case, an initial vehicle acceleration of 3 m/sec² was obtained. In the intermediate and high-speed regions, being limited by equation (9) in accordance with the relation between DC voltage and motor terminal voltage, the torque which can be generated decreases with increasing rotational speed. Here, the rotational speed range in which the maximum torque can be maintained during driving operation in largely influenced by the internal resistance of the battery. If the internal resistance of the battery were equal to zero, then the maximum torque could be maintained up to the vicinity of the rated rotational frequency.

By applying field-weakening control from the instant when the rated rotational speed (1283 rpm at 150 km/h) is exceeded, the elevation of motor voltage is suppressed, and the operating range is extended to 1540 rpm (at 180 km/h). During the control process, the maximum braking torque is limited to the value (22.5 kgm) equivalent to the practical deceleration of 1.5 m/sec².

Figure 7 shows the calculated and actual measured values of the overall efficiency characteristic plotted against output. At the rated rotational speed (1283 rpm), the overall efficiency exceeded 92%, and a similar level of efficiency was also observed in the region of field weakening control (1540 rpm). Although the efficiency was calculated
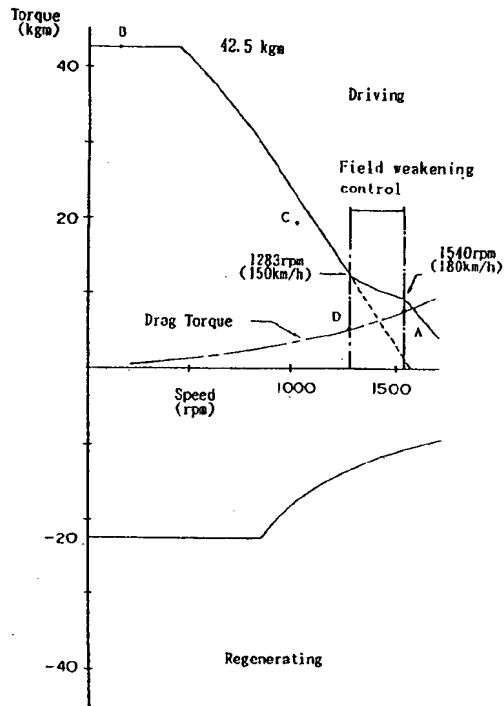
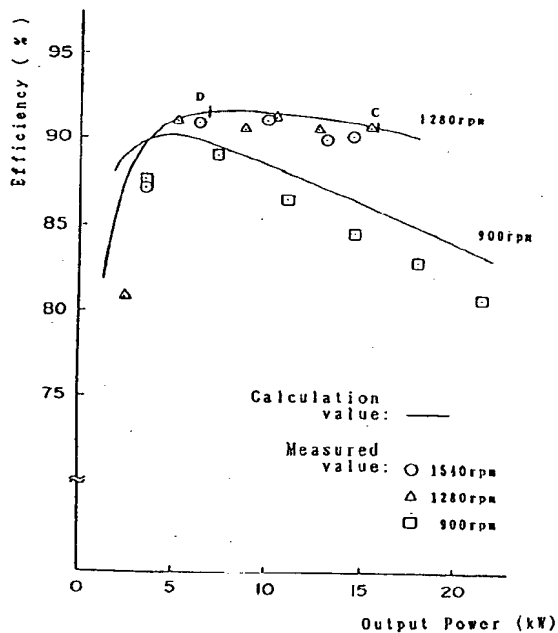Fig. 6    Rotational speed vs maximum torque characteristics



Fig.7    Overall efficiency characteristics

considering only fundamental wave losses and neglecting harmonics losses, the measured efficiency agrees well with the calculated value.    Harmonics losses were negligible

because the harmonic currents were small.

### 4.3 Simulation studies of traveling range per charge

One of the important performance specifications of the IZA is the traveling range, as shown in Table 1. The other specifications such as maximum speed and acceleration time can be calculated with comparative ease, because these characteristics depend only upon the torque of the motors, the running resistance, and the inertia of vehicle.    On the other hand, calculation of traveling range is more complex, especially for pattern mode operation.    This problem was studied by simulation [8].

The traveling ranges when the vehicle is driven at constant speeds of 40 km/h and 100 km/h were calculated as 556.7 km and 271.7 km, respectively. The efficiency of the motor drive system at 40 km/h is 78.0%,   lower than the efficiency of 83.6% at 100 km/h.   This is because the IZA was designed to drive at a speed higher than 100 km/h.    The regeneration technology that returns kinetic energy to the battery in the braking mode is very important in decreasing the energy consumption of an electric vehicle.    The four mode operating pattern is ordinarily used to assess the effects of regeneration.    The simulated traveling ranges for four mode operation with and without regeneration were 231.8 and 192.8, respectively;  Figure 8 shows the respective energy consumption values in percentage of total energy of without regeneration mode.    The motor and inverter losses increase in the regenerative mode as compared with the non-regenerative mode, because the motor and inverter currents increase.    Since the kinetic energy at low speeds is smaller than the energy losses in the motor and inverter, only mechanical braking is employed at speeds less than 10 km/h. Consequently, the regeneration efficiency of the drive system, including the motor, inverter, and battery, is about 52 percent in the braking mode.  In the constant speed mode, 78.0 and 83.6 percent of the energy at 40km/h and 100km/h respectively are consumed by rolling resistance and aerodynamic drag, this being the energy which actually drives the vehicle.    From Figure 8, one can calculate that 60.9 percent of the energy in four mode operation is consumed by motor and inverter losses.    This fact suggests the importance of enhancing the efficiency of the motor and inverter in order to improve the   traveling range for urban driving.

### 5.    Vehicle performance tests

The newly developed motors and motor controllers were finally installed in the electric vehicle IZA and their performance was evaluated by vehicle transit tests.
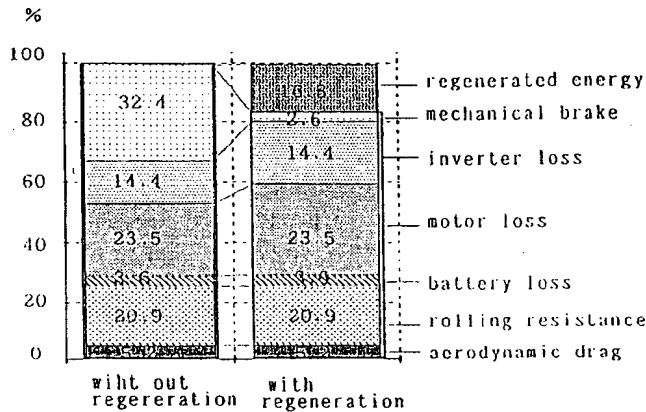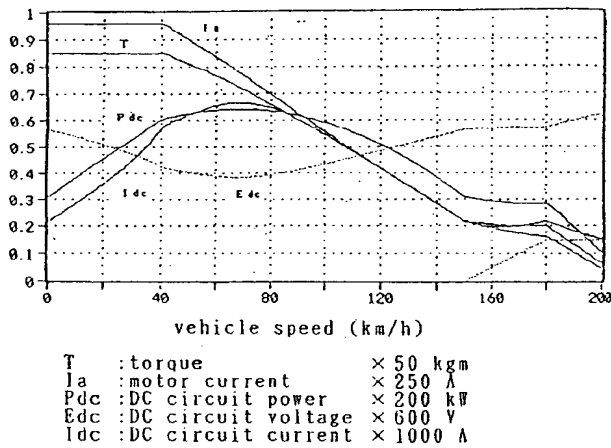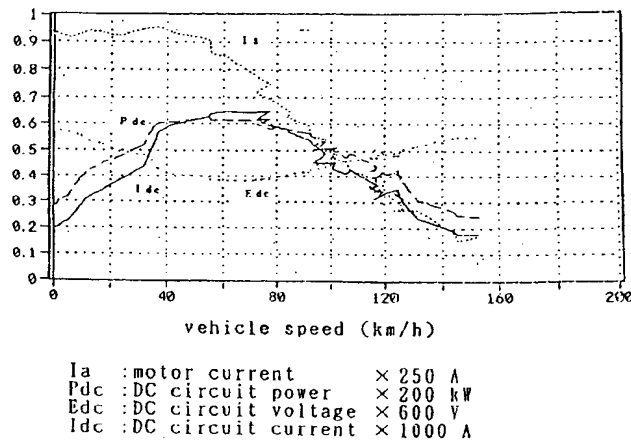
25

Fig.8 Simulated energy consumption at four mode operation



T    : torque            × 50 kgm
Ia   : motor current     × 250 A
Pdc  : DC circuit power   × 200 kW
Edc  : DC circuit voltage × 600 V
Idc  : DC circuit current × 1000 A

(a) simulated result



Ia   : motor current     × 250 A
Pdc  : DC circuit power   × 200 kW
Edc  : DC circuit voltage × 600 V
Idc  : DC circuit current × 1000 A

(b) measured values during the acceleration test

Fig.9  Dynamic characteristics of driving system

| Speed    (km/h) | 0 | 10 | 20 | 30 | 40 | 100 |
|---|---|---|---|---|---|---|
| Running resistance (N) (Converted into Torque) | 99 | 107 | 118 | 135 | 150 | 328 |

TABLE 3 Values of running resistance

| Item | Constant speed of 40km/h (km) | Constant speed of 100km/h (km) | Four mode operation (km) |
|---|---|---|---|
| Measured range | 548 | 270 | 239 |
| Result of simulation | 556.7 | 271.7 | 231.8 |

TABLE 4 Traveling range per charge

The maximum speed and acceleration of the IZA were tested on the JARI test course on the condition of a wind velocity of 1.2 m/s against. The maximum speed was measured as 176 km/h, nearly equal to the target value of 180 km/h. Acceleration time from zero to 400 m was measured as 18.05 seconds, and was also virtually equal to the target value of 18 seconds. The dynamic torque - speed characteristic of the drive system measured through the aforesaid acceleration test was compared with the simulated characteristic. Simulated maximum values of parameters such as torque, motor current, and DC power for given vehicle speeds in the accelerating state are shown in Figure 9(a), while Figure 9(b) shows measured values obtained by collecting data only when the accelerator petal was fully depressed during the acceleration test, which means that maximum torque is commanded. The characteristics in these two figures show excellent agreement, confirming that the motor drive system actually performed as designed.

The traveling range per charge of the IZA was measured with the vehicle mounted on a chassis dynamometer. The parameters such as curb weight, aerodynamic drag, and rolling resistance used in this test had been previously measured [9]. The curb weight is 1660 kg, and the values of the running resistance for the respective speeds are shown in Table 3. Table 4 shows both the measured and simulated traveling ranges for constant speeds of 40 km/h and 100 km/h as well as four mode operation, and the measured traveling ranges agree well with the results of simulation.

6. Conclusion

The present paper has described the in-wheel motor and controller employed in the high-performance electric vehicle IZA, as well as the characteristics of the driving system and the results of evaluation tests. In conclusion,
(1) The IZA requires large torque outputs from the in-wheel motor, and since the size of the motor is severely restricted, we developed a novel synchronous motor with an SmCo magnet which achieves this purpose. We have described the structure of this motor, which was designed and fabricated after detailed analysis of the magnetic circuit.
(2) In order to satisfy the specifications of the IZA, rapid-

response sinusoidal current control and torque control with an IGBT inverter have been developed. Although synchronous motors have high efficiency, the margin of torque control in the high speed region is ordinarily small because of higher induced motor voltage. In the present system, a maximum speed of 176 km/h has been achieved by the use of field weakening control.

(3) In order to achieve wide range torque and speed control, the control system must be designed taking the characteristics of the battery as well as the losses of the semiconductor devices and the motor losses into consideration, The total speed-torque characteristic has been deduced taking the motor, inverter, and battery into consideration, and this characteristic has been confirmed by 0-4兆 m acceleration tests.

(4) The traveling ranges in the constant speed mode and the pattern operating mode were analyzed and the details of energy consumption were studied.

Various evaluation tests confirmed that the performance of the motor, inverter and driving system almost fully attained the design targets.

REFERENCES

[1]Agency for Industrial Science and Technology, MITI: "Research and Development Work on Electric Vehicles" (in Japanese), 1977

[2]J.S.Dunning : "Electric Vehicles and Battery Technology" Proceedings of 1990 International Symposium on Low-Pollution Vehicles, p.13, 1990

[3]N. Irie et al.: "Nissan FEV-A: A New Concept Electric Vehicle" Proceedings of EVS.11, No.13.02, 1992

[4]Y. Kaya, H.Ishitani et al.: "Research and Development Project for An Advanced Electric Vehicle, IZA" Proceedings of EVS.11, No.5.03, 1992

[5]M. Terashima et al.: "Drive System with 4 In-Wheel Motors for Electric Vehicle" 6th Annual Conference of IEE Japan-IAS(JIASC)

[6]M. Terashima et al.: "AC Drive System with 4 In-Wheel Motor for High Performance Electric Vehicle" (in Japanese), Transactions of IEE Japan, Vol.114-D, No.1, p33, 1994

[7]K. Shinohara et al.;"Performance Analysis of Permanent Magnet AC Servo Motor Driven by Current Controlled PWM Inverter" (in Japanese), Transactions of IEE Japan, Vol.110-D, No.10, p1081, 1990

[8]H. Shimizu, Y. Iikura et al.; "A Simulation Program for the Design and Evaluation of a High Performance Electric Vehicle" (in Japanese), Journal of the Japan Society for Simulation Technology, Vol.10, No.3, p63, 1991

[9]M.Ono et al.; "Development of the Chassis, Suspension, and Body of the Advanced Electric Vehicle IZA" Proceedings of EVS.11, No.5.06, 1992